

28 **ABSTRACT**

29 Root hair initiation is a highly regulated aspect of root development. The plant hormone, ethylene, and its
30 precursor, 1-amino-cyclopropane-1-carboxylic acid (ACC), induce formation and elongation of root hairs.
31 Using confocal microscopy paired with redox biosensors and dyes, we demonstrated that treatments that
32 elevate ethylene levels led to increased hydrogen peroxide accumulation in hair cells prior to root hair
33 formation. In two ethylene-insensitive mutants, *etr1-3* and *ein3/eil1*, there was no increase in root hair
34 number or ROS accumulation. Conversely, *etr1-7*, a constitutive ethylene signaling receptor mutant, has
35 increased root hair formation and ROS accumulation like ethylene-treated Col-0 seedlings. The *caprice* and
36 *werewolf* transcription factor mutants have decreased and elevated ROS levels, which are correlated with
37 levels of root hair initiation. The *rhd2-6* mutant, with a defect in the gene encoding a ROS synthesizing
38 Respiratory Burst Oxidase Homolog C (RBOHC) and the *prx44-2* mutant defective in a class III peroxidase,
39 showed impaired ethylene-dependent ROS synthesis and root hair formation and EIN3/EIL1 dependent
40 transcriptional regulation. Together, these results indicate that ethylene increases ROS accumulation
41 through RBOHC and PRX44 to drive root hair formation.

42

43 **SUMMARY STATEMENT**

44 The gaseous hormone ethylene increases root hair initiation by elevating reactive oxygen species (ROS) in
45 trichoblast cells. Genetic and biochemical approaches identified ethylene-regulated ROS producing
46 enzymes that drive root hair initiation.

47 INTRODUCTION

48 The initiation of root hairs is genetically programmed and environmentally sensitive, making them
49 an ideal model for studying single cell differentiation in plants. Root hairs are single-cell extensions that
50 differentiate from longitudinal epidermal cell files, known as trichoblasts (Leavitt, 1904; Salazar-Henao et
51 al., 2016). The formation of root hairs is modulated by environmental changes to increase root surface area
52 to allow for efficient water and nutrient uptake (Bruex et al., 2012), while also anchoring plants in soil to
53 reduce erosion (De Baets et al., 2020). In *Arabidopsis*, the root epidermis consists of an alternating pattern
54 of trichoblasts, which form root hairs, and atrichoblasts, which are non-hair forming cells (Pemberton et
55 al., 2001; Salazar-Henao et al., 2016). Root hair formation is dictated by cell positioning; epidermal cells
56 overlying two cortical cells can become hair forming cells, while those overlying one cortical cell will
57 become non-hair cells (Berger et al., 1998; Salazar-Henao et al., 2016). Root hair development is separated
58 into two processes: root hair initiation and root hair elongation (Dolan et al., 1994). A recent report divided
59 this process into 10 precise stages and examined the molecular mechanisms that drive this process. During
60 stages -7 to -1, RHO Of Plants (ROP) proteins (ROP2, ROP4, and ROP6) and ROP Guanine Nucleotide
61 Exchange factors (ROP GEFs) that regulate ROP activity accumulate at the future site of initiation
62 (Denninger et al., 2019; Molendijk et al., 2001), this is followed by polymerization of actin filaments along
63 which vesicles move to deposit membrane needed for polarized tip growth (Salazar-Henao et al., 2016).
64 During tip growth, tip focused reactive oxygen species (ROS) (Foreman et al., 2003; Gayomba and Muday,
65 2020; Monshausen et al., 2007) and Ca^{2+} gradients (Carroll et al., 1998) have been identified to drive
66 exocytosis of the cell wall and membrane materials driving subsequent root hair elongation. These
67 processes are separable as mutants with either impaired root hair initiation or elongation have been
68 identified (Masucci and Schiefelbein, 1994; Schiefelbein and Somerville, 1990).

69 Genetic screens in *Arabidopsis thaliana* have provided a wealth of insight into the proteins that
70 drive root hair development (Lee and Schiefelbein, 1999; Masucci and Schiefelbein, 1996; Rerie et al.,
71 1994). For example, the mutants *transparent testa glabra* (*ttg*), *glabra2* (*gl2*), and *werewolf* (*wer*) have root
72 hairs that form from both trichoblast and atrichoblast cells (Di Cristina et al., 1996; Galway et al., 1994;
73 Lee and Schiefelbein, 1999). Many of the protein products of these mutants have been mapped to
74 transcriptional cascades that drive root hair differentiation (Shibata and Sugimoto, 2019) and have been
75 shown to localize prior to root hair initiation (Denninger et al., 2019). In non-hair cells, a transcriptional
76 complex comprised of three transcription factors (TFs), WER, GLABRA 3 (GL3) or its functionally
77 redundant ENHANCER OF GLABRA (EGL3), and TTG1, function as a transcriptional activator of the
78 GL2 protein, which leads to repression of root hair initiation (Grebe, 2012; Salazar-Henao et al., 2016). In
79 trichoblasts, *WER* expression is repressed, which allows for the formation of an alternate transcriptional

80 complex comprised of CAPRICE (CPC) or the functionally redundant proteins ENHANCER OF TRY
81 AND CPC1 (ETC1), ETC3, or TRYPTICHON (TRY) (Schiefelbein et al., 2014). When this pathway is
82 active, GL2 is not expressed and root hair initiation proceeds (Salazar-Henao et al., 2016).

83 Another genetic screen identified the *root hair defective* (*rhd*) mutants which have impaired root
84 hair initiation, elongation, or structure (Masucci and Schiefelbein, 1994; Schiefelbein and Somerville,
85 1990). The mutation in *rhd2*, was mapped to the *RBOHC* (respiratory burst oxidase homolog C/NADPH
86 oxidase) gene (Foreman et al., 2003). The *rhd2* mutant was identified for altered root hair elongation
87 (Schiefelbein and Somerville, 1990), but was recently reported to also have impaired root hair initiation
88 (Gayomba and Muday, 2020). RBOHs are integral plasma membrane proteins that produce superoxide,
89 which can be dismutated to hydrogen peroxide via superoxide dismutase (SOD) or other non-enzymatic
90 mechanisms (Chapman et al., 2019). H₂O₂ can then enter into the cell through aquaporins (Bienert et al.,
91 2007), where it can act as a signaling molecule to drive cellular processes. Signaling induced ROS regulates
92 protein function by reversibly oxidizing cysteine residues to sulfenic acids (Cys-SOH) (Poole and
93 Schoneich, 2015).

94 There are 10 RBOH family members (RBOHA-RBOHJ) in Arabidopsis and each play distinct roles
95 in organ development and stress response (Chapman et al., 2019). RBOHs can be regulated transcriptionally
96 or enzymatically by a number of mechanisms, including calcium binding, phosphorylation, and
97 phosphatidic acid binding (Kobayashi et al., 2007; Postiglione and Muday, 2020; Suzuki et al., 2011).
98 RBOH-induced ROS production is also regulated by hormone signaling, as many plant hormones generate
99 ROS as a mechanism to drive growth and developmental processes (Chapman et al., 2019; Kwak et al.,
100 2003; Mittler et al., 2011; Postiglione and Muday, 2020); For example, abscisic acid (ABA), a hormone
101 involved in abiotic stress response, has been shown to induce RBOH-derived ROS production to prevent
102 water loss in leaves (Kwak et al., 2003). Auxin induces root hair initiation (Gayomba and Muday, 2020)
103 and elongation (Mangano et al., 2017) through a localized increase in ROS, suggesting that RBOH may
104 drive hormone induced root hair elongation.

105 The plant hormone ethylene enhances root hair initiation and elongation. Treatment with ethylene,
106 or its precursor 1-amino-cyclopropane-1-carboxylic acid (ACC), leads to proliferation of root hairs, with
107 substantial increases in their length (Tanimoto et al., 1995). The ethylene induction of root hairs occurs
108 through the canonical ethylene signaling pathway, which is initiated when ethylene binds to one of the five
109 receptors, ETR1, ERS1, ETR2, ERS2, or EIN4 (Binder, 2020; Bleecker, 1999). When ethylene is absent,
110 the receptors are in the “on state” leading to activation of the CTR1 Raf-like kinase (Kieber et al., 1993);
111 this turns the pathway off via phosphorylation and subsequent degradation of the EIN2 transmembrane
112 protein (Alonso et al., 1999; Ju et al., 2012). When ethylene binds to its receptors they shift to the “off state”

113 which prevents activation of CTR1. This allows for cleavage and translocation of the EIN2 C-terminus into
114 the nucleus (Ju et al., 2012; Wen et al., 2012) where it stabilizes the EIN3/EIL1 TFs leading to ethylene
115 responsive gene expression. Previous work has shown that ethylene regulates root hair elongation through
116 the EIN3 transcription factor (Feng et al., 2017) and that EIN3 also controls the formation of ectopic root
117 hairs when ethylene reaches very high levels (Qiu et al., 2021). EIN3 physically interacts with RHD6, a
118 positive regulator of root hair development, to form a transcriptional complex that binds to and induces
119 expression of *RSL4* resulting in increased root hair elongation (Feng et al., 2017). However, the mechanistic
120 events that drive ethylene-induced root hair initiation have not been fully described and the role of ROS as
121 a downstream molecule in ethylene-induced root hair development has not been reported.

122 This work asked whether ethylene acts to increase ROS levels to drive root hair initiation.
123 Fluorescent dyes and biosensors that report ROS levels were used to examine ROS accumulation after
124 ethylene or ACC treatment in trichoblast cells in the differentiation zone. This response was shown to be
125 dependent on ETR1 receptor activity and EIN3 TF activity. The role of RBOHC and class III peroxidase
126 enzymes in ethylene-dependent ROS synthesis was demonstrated using mutants in genes encoding these
127 ROS generating enzymes. Together these experiments demonstrated that ROS is a signaling molecule in
128 ethylene induced root hair formation and identified several enzymes that participate in producing ethylene-
129 induced ROS.

130 RESULTS

131 Root hair numbers increases in ACC treated roots

132 The role of ethylene signaling in root hair initiation was examined by testing the effects of short-
133 term treatments with the ethylene precursor, ACC, on the number and position of root hairs in 5-day old
134 seedlings. Root hairs were visualized in wild type (Col-0) seedlings grown in the presence of 0.7 μM ACC
135 for 4 hours (Fig. 1A). The root tip was divided into three 500 μm zones starting from the root tip and the
136 number of initiated root hairs formed in each zone was quantified Fig. 1B). We defined root hair initiation
137 as root hairs that were at stage +2 and above as described previously (Denninger et al., 2019). In zone 1,
138 root hairs did not form in either untreated or ACC-treated seedlings. In zone 2, there were very few root
139 hairs in untreated roots, however, ACC-treatment increased the number of root hairs by 10-fold. There was
140 also a 2-fold increase in root hair number in zone 3 of ACC-treated seedlings compared to untreated
141 controls. This dose of ACC does not cause ectopic root hair formation in non-hair cells, but rather increased
142 the number of hair cells forming root hairs in these two zones. It is also evident from Fig. 1, that this
143 treatment increased the length of root hairs in both zone 2 and 3, consistent with prior reports (Feng et al.,
144 2017; Harkey et al., 2018). These data suggest that ACC-induced root hair initiation begins between 500
145 and 1000 μM from the root tip. Therefore, to understand the mechanisms driving the process of root hair
146 initiation our experiments focused on this region.

147 Long term ACC and ethylene treatment also result in a shorter primary root due to reduced
148 elongation of root cells, so we examined whether the effect on root hair initiation was the result of altered
149 length (Harkey et al., 2018). The effect of 4 hours of treatment with low doses of ACC (0.7 μM) on root
150 elongation were examined. Primary roots were stained with the cell wall specific dye, propidium iodide
151 (PI). We then measured the length of 5 epidermal cells from 6-8 roots per treatment condition, measuring
152 the length of cells at either end and in the middle of zone 2 (designated zone 2A, 2B, and 2C in Fig. S1).
153 There was no difference in cell length in any of these 3 regions after 4 hours of ACC treatment compared
154 to untreated controls. These results are consistent with short term and low dose ACC treatments increasing
155 root hair number by inducing root hair formation from trichoblasts in zone 2, rather than as an indirect
156 effect of a shorter primary root.

157 A ROS dependent transcriptional reporter increases in ACC treated roots

158 We asked whether ethylene leads to elevated reactive oxygen species (ROS) to drive ethylene-
159 induced root hair initiation. ROS dependent gene expression along the root was examined using the
160 ZAT12p-ROS ratiometric biosensor (Lim et al., 2019). This reporter construct contains the promoter of the
161 ROS sensitive transcription factor, *ZAT12*, driving GFP and the constitutive ubiquitin10 promoter driving

162 mCherry. We compared the fluorescent signal of *ZAT12p*-GFP in the presence and absence of ACC as
163 visualized by laser scanning confocal microscopy (LSCM), with GFP reported as green and mCherry
164 reported as magenta (Fig. 1C). The ratio of signal of GFP (green) to mCherry was quantified across the
165 entire root as a distance from the root tip. In ACC-treated roots, the GFP/mCherry ratio increased beginning
166 at approximately 500 μm from the root tip, which corresponded to zone 2, where root hair induction was
167 maximal upon treatment with ACC (Fig. 1D). To examine the possibility that the *ZAT12* promoter is
168 ethylene regulated (rather than being ROS regulated), we examined transcriptomic datasets in which roots
169 were treated with ACC or ethylene (Harkey et al., 2018). These three data sets do not show ACC or
170 ethylene-driven transcriptional changes in *ZAT12* transcript abundance.

171 **Ethylene increases the signal of the H₂O₂ selective dye, Peroxy Orange1, in trichoblast cells**

172 The hydrogen peroxide selective dye, Peroxy-Orange 1 (PO1), was used to determine whether there
173 were cell type-specific increases in ROS in response to treatment with ACC or ethylene gas. PO1 is a
174 permeable, boronate-based dye that is non-fluorescent in its reduced form, but becomes fluorescent when
175 irreversibly oxidized by H₂O₂ (Dickinson et al., 2010). Col-0 seedlings were treated with either 0.7 μM
176 ACC or 0.05 ppm of ethylene gas for 4 hours followed by PO1 staining. In Col-0 roots, PO1 fluorescence
177 was visualized using LSCM in zone 2 of roots treated with control, ACC, or ethylene gas for 4 hours (Fig.
178 2). In Arabidopsis, root hairs form in alternating patterns, so that every root hair forming cell (trichoblast)
179 is adjacent to a non-hair cell (atrachoblast). We quantified ROS accumulation by analyzing PO1 signal after
180 confocal imaging, by drawing a line across the width of the root that spans 5 epidermal cell files so that the
181 PO1 signal in 3 trichoblasts (numbered 1, 3, and 5) and 2 atrachoblasts (numbered 2 and 4) was quantified
182 (Fig. 2A).

183 We found that PO1 accumulation in trichoblasts in zone 2 of untreated seedlings was slightly, but
184 not significantly higher than atrachoblasts. In trichoblast cells of ACC and ethylene treated seedlings, there
185 was a significant increase in PO1 accumulation compared to trichoblasts of untreated seedlings. In contrast,
186 there were no changes in PO1 in the atrachoblasts suggesting that ethylene and ACC treatment increased
187 ROS levels in only the cells that formed root hairs, with PO1 fluorescence intensity values in trichoblasts
188 after both treatments showing the same magnitude increase as roots treated with ACC (Fig. 2B). These
189 results are consistent with this short term and low dose treatment with ACC leading to efficient conversion
190 to ethylene that in turn produces elevated ROS in trichoblast cells (Fig. 2B). This is in contrast with some
191 studies in which other developmental processes are altered by ACC acting directly, rather than conversion
192 to ethylene (Li et al., 2021).

193 **ROS accumulation increases prior to root hair emergence**

194 To determine whether ethylene-induced ROS accumulation drives root hair emergence, we asked
195 whether ACC-induced ROS increases were detectable prior to the first ACC-induced root hair initiation.
196 Wild type Col-0 seedlings were treated with ACC for either 2 or 4 hours and PO1 fluorescence was
197 visualized in trichoblasts that did not have a root hair bulge (stages below +1) (Fig. 3A). This PO1 signal
198 is only reported in the 2-hour ACC treatment, as there were insufficient number of cells without root hair
199 bulges to quantify in root treated for 4 hours. Total PO1 accumulation was measured in 5 individual
200 trichoblasts per root treated with and without ACC. Signal was quantified across the area of the entire cell
201 and the average PO1 intensity of 24-30 individual cells was reported (Fig. 3B). Atrichoblast signal was not
202 quantified as ROS levels did not change in those cells (Fig. 2B). These data showed a 1.3-fold increase in
203 PO1 accumulation in hair cells of seedlings treated with ACC for 2h as compared to untreated controls,
204 when trichoblast cells that had not yet begun to initiate root hairs were examined. These data are consistent
205 with the hypothesis that ROS acts as a driver of root hair initiation downstream of ethylene signaling.

206 **Ethylene signaling mutants show altered ROS accumulation patterns and root hair phenotypes**

207 The ethylene signaling pathway is well defined (Fig. 4A) and mutants in key signaling proteins,
208 including receptors and transcription factors are available. ROS accumulation was examined in response to
209 ACC treatment in these ethylene signaling mutants to ask whether this response was dependent on the
210 ethylene signaling pathway and downstream transcriptional responses. The number of root hairs and
211 average length were previously reported in loss-of-function and gain-of-function ethylene receptor mutants,
212 *etr1-7* and *etr1-3*, and the transcription factor mutant *ein3eill* in the presence and absence of ACC treatment
213 (Harkey et al., 2018). *etr1-7* is a LOF mutant in which the ETR1 receptor is inactive, therefore the ethylene
214 signaling pathway is constitutively signaling and there are increased numbers of root hairs independent of
215 ACC addition, while *etr1-3* is a GOF mutant in which the ETR1 receptor is always active leading to the
216 ethylene signaling pathway being inhibited (Harkey et al., 2018; Hua and Meyerowitz, 1998). The double
217 mutant *ein3eill* has mutations in genes encoding EIN3 and EIL1 TFs (Chao et al., 1997; Solano et al.,
218 1998). Both *etr1-3* and *ein3eill* have reduced root hair initiation in response to ACC treatment (Harkey et
219 al., 2018). We examined the PO1 distribution patterns in root hair cells with and without ACC treatment in
220 these three mutants.

221 We visualized PO1 fluorescence via LSCM and saw that the constitutive ethylene signaling mutant
222 *etr1-7* had increased H₂O₂ in root hair cells and an increased number of trichoblasts with emerged root hairs
223 regardless of ACC treatment (Fig. 4B). The PO1 signal in *etr1-7* in the absence of ACC is significantly
224 elevated over untreated Col-0, but is equivalent to ACC treated Col, and is not significantly changed by
225 ACC treatment. The opposite response was seen in the ethylene-insensitive *etr1-3* and *ein3eill* mutants, as
226 they showed no change in PO1 signal in response to ACC treatment, resulting in a significantly lower level

227 than ACC treated Col-0 and no induction of root hair initiation. Together, these results suggest that the
228 ETR1 receptor and EIN3/EIL1 TFs are required for ACC-induced ROS accumulation and root hair
229 initiation and suggesting that in these experiments ACC is acting via conversion to ethylene.

230 **Mutants with altered root hair formation also show altered ROS accumulation**

231 We also examined the effect of mutations that alter root hair formation on ROS levels. The
232 *werewolf* (*wer*) mutant has increased root hair formation, while the *caprice* (*cpc*) mutant with decreased
233 root hair formation. ROS accumulation was significantly higher in root hairs along the root in *wer* compared
234 to both Col-0 and *cpc*, while *cpc* had significantly less ROS accumulation along the root compared to Col-
235 0 (Fig. 5).

236 **The RBOHC knockout mutant, *rhd2-6*, shows decreased ROS accumulation after ACC treatment**

237 It has been previously reported that the respiratory burst oxidase homolog C (RBOHC) is involved
238 in ROS production and subsequent root hair elongation (Foreman et al., 2003). We have also shown that
239 there is decreased ROS in root hairs of the *rhd2-6* mutant, which has an insertion mutation in the *RBOHC*
240 gene (Gayomba and Muday, 2020). Therefore, we asked whether RBOHC is required for ACC-induced
241 ROS increases and root hair initiation. We examined root hair numbers via light microscopy in ACC-treated
242 *rhd2-6* (*rbohc*) seedlings (Fig. 6). Root hair number in the ACC-treated *rhd2-6* mutant was significantly
243 less than ACC-treated Col-0, suggesting that RBOHC contributes to ethylene-induced root hair initiation
244 (Fig. 6B). We also quantified the length of all root hairs in Zone 2 using the segmented line tool in ImageJ.
245 A histogram showing the distribution of lengths of root hairs (reported as percentage in each length bin out
246 of total number of roots) revealed that the length of root hairs increased after ACC treatment and that the
247 *rhd2-6* mutant has reduced root hair elongation in the presence of ACC relative to Col-0.

248 We also visualized the PO1 fluorescence by LSCM in the *rhd2-6* mutant with and without ACC
249 treatment (Fig. 6D). We report the average of 2 trichoblast cells (1 and 5 from Fig. 2) and two atrichoblast
250 cells (2 and 4) in Fig. 6E. This reveals a significant increase in H₂O₂ fluorescence accumulation in Col-0
251 hair cells, while in *rhd2-6* there is no significant increase after ACC treatment (Fig. 6E), suggesting that
252 RBOHC contributes to ethylene-induced ROS accumulation. The data is reported for all 5 cell files in Fig.s
253 S2. These images reveal slight increases in numbers of root hairs in ACC-treated *rhd2-6* roots, suggesting
254 that the ACC also acts to induce root hairs in an RBOHC-independent mechanism.

255 As there are also other RBOH enzymes expressed in roots, we asked whether these other enzymes
256 affect root hair formation. RBOHD and RBOHF are highly expressed in roots and have been shown to be
257 involved in regulation of root elongation and lateral root development (Chapman et al 2019). Therefore, to

258 determine these other root expressed RBOHs contributed to ethylene-induced ROS accumulation, PO1
259 accumulation patterns were examined in the *rbohdf* double mutant and compared to *rhd2-6*. No change
260 was seen in ROS levels in hair cells of *rbohdf*, suggesting that these RBOHs do not contribute to ethylene-
261 induced ROS synthesis in root hair cells (Fig. S2).

262 **RBOH transcript abundance and enzyme activity increases in response to ethylene signaling**

263 Elevated ethylene may either increase *RBOHC* transcript abundance or enzyme activity. We
264 examined several transcriptomic datasets with ACC or ethylene treated roots and found a subtle change in
265 the *RBOHC* transcripts, but not significant enough to pass the filtering on this transcriptomic analysis
266 (Harkey et al., 2018; Harkey et al., 2019) (Table S1). However, we also performed qRT-PCR in Col-0 and
267 *ein3eill* treated with and without ACC to examine changes in abundance in the transcript encoding
268 RBOHC. *RBOHC* transcript abundance was 2-fold higher in Col-0 treated with ACC compared to Col-0
269 controls. The levels of *RBOHC* transcript abundance in untreated *ein3eill* were equivalent to Col-0, while
270 and the increase by ACC treatment in Col-0 was lost in *ein3eill* (Fig. S3B). To determine if ethylene
271 signaling regulated RBOH enzyme activity, a spectrophotometric assay using nitro blue tetrazolium (NBT)
272 dye as an electron acceptor, was performed. NBT is reduced by superoxide to monoformazan and this
273 reduction can be detected at 530 nm. This experiment was performed in protein extracts from 7-day old
274 roots of Col-0 and *rhd2-6* treated with and without ACC for 4 hours. Older roots were used in this
275 experiment to obtain an adequate amount of protein for these assays. There was a significant 2-fold increase
276 in monoformazan production in protein extracts of Col-0 roots treated with ACC for 4 hours compared to
277 controls (Fig. 6F). The enzyme activity of roots of *rbohcrhd2-6* was 3-fold lower in both control and ACC
278 treated conditions than roots of similarly treated Col-0 (Fig. 6F). These data are consistent with previous
279 results indicating that the RBOHC enzyme constitutes the majority of the RBOH activity in roots (Chapman
280 et al., 2019; Gayomba and Muday, 2020).

281 **Transcription of *PRX44* increases with ACC treatment driving ROS accumulation and ethylene- 282 induced root hair initiation**

283 The *ein3/eill* transcription factor mutant has reduced root hair initiation and a reduction in PO1
284 signal in trichoblasts suggesting that there is transcriptional regulation of ROS producing enzymes that
285 drive root hair initiation. We examined a previously published microarray time course experiment in roots
286 treated with ACC (Harkey et al., 2018), to identify candidate transcriptional targets profiling the expression
287 pattern of transcripts encoding both ROS producing enzymes and proteins linked to trichoblast cell
288 specification. ROP2, ROPGEF3, ROPGEF4, GL2, RSL4 and RHD6, which are linked to root hair initiation
289 (Denninger et al., 2019), showed no transcriptional response to ACC treatment and primers that recognize

290 RSL1 and RSL2 are not present on the microarray and could not be examined in this dataset (Table S1).
291 This transcriptomic analysis did not identify the previously reported ethylene induction of RSL4 (Feng et
292 al., 2017), which was revealed with high dose treatment of ethylene that led to ectopic root hair formation
293 from non-hair cells, suggesting the RSL4 transcript changes may be dose dependent or ethylene specific.
294 A number of transcripts encoding class III peroxidases (PRXs) changed in abundance in response to ACC,
295 including the transcript encoding *PRX44*, which increased by 3-fold. Class III peroxidases are specific to
296 plants and exist in large multigene families. They have been implicated in root hair tip growth, as null
297 mutants have shorter root hairs compared to wild type (Mangano et al., 2017). Recent work has shown that
298 auxin induces expression of genes encoding four class III peroxidases (PRX), which results in an increase
299 in both root hair length and ROS accumulation (Mangano et al., 2017), however, the role of ethylene
300 signaling in regulating class III PRX expression to modulate root hair initiation or elongation has not been
301 reported.

302 We examined control and ACC-treated seedlings harboring the *PRX44* promoter driving GFP and
303 examined GFP expression via LSCM. Seedlings treated with ACC showed a statistically significant >2-
304 fold increase in GFP fluorescence, suggesting that the *PRX44* promoter is induced downstream of ethylene
305 signaling (Fig. 7A-B). qRT-PCR was also performed in Col-0 and *ein3eill* treated with and without ACC
306 to examine changes in abundance in the transcript encoding PRX44. We found that there was a 2-fold
307 increase in *PRX44* transcript abundance in Col-0 treated with ACC compared to Col-0 controls. We also
308 found that there was a significant decrease in *PRX44* transcript abundance in untreated and ACC treated
309 *ein3eill* compared to Col-0 (Fig. S3A). We also asked whether these peroxidases participate in ACC-
310 regulated root hair initiation. We examined root hair numbers via light microscopy in Col-0 and *prx44-2*
311 seedlings treated with and without ACC. The number of root hairs formed in the *prx44-2* mutant treated
312 with ACC was significantly less than in ACC treated Col-0 (Fig. 7C-D). The root hairs in the ACC-treated
313 mutant were also significantly shorter compared to Col-0, which is consistent with the phenotype that has
314 been reported in response to auxin treatment (Fig. 7E) (Mangano et al., 2017). When PO1 accumulation
315 patterns were examined via LSCM, we observed no significant increase in PO1 accumulation in hair cells
316 of *prx44-2* seedlings treated with ACC (Fig. 7F-G). We also examined *prx73-4*, since transcripts encoding
317 PRX73 have been reported to be induced with auxin treatment to drive root hair elongation (Mangano et
318 al., 2017) and these transcripts increased in abundance in response to ACC treatment (Table S1). When
319 treated with ACC, the *prx73-4* mutant exhibited root hair initiation and ROS accumulation patterns that
320 were similar to wild-type seedlings, suggesting that this class III PRX is not involved in ethylene-induced
321 ROS synthesis and root hair initiation. These combined data indicate that both the class III PRX44 and
322 PRX73 are transcriptionally regulated by ethylene, but only PRX44 contributes to ethylene induced ROS
323 accumulation in root hairs and root hair initiation.

324

325 DISCUSSION

326 Ethylene is a key hormonal regulator of root hair initiation and elongation (Guzman and Ecker,
327 1990; Kieber et al., 1993). Although the proteins that drive ethylene signaling are well characterized, the
328 downstream proteins that control the root hair developmental processes have received less attention.
329 Reactive oxygen species (ROS) are critical for both root hair initiation and elongation (Foreman et al.,
330 2003; Gayomba and Muday, 2020). In root hairs, one source of ROS is the NADPH oxidase
331 (NOX)/respiratory burst oxidase homolog C (RBOHC) that is localized to root hairs to facilitate cell wall
332 loosening and subsequent tip focused Ca^{2+} accumulation leading to root hair cell elongation (Foreman et
333 al., 2003; Monshausen et al., 2007). The plant hormone auxin also increases ROS accumulation to drive
334 root hair elongation (Mangano et al., 2017), suggesting that ROS could also act as a signaling molecule in
335 ethylene-induced root hair initiation and elongation (Foreman et al., 2003; Gayomba and Muday, 2020;
336 Jones et al., 2007; Takeda et al., 2008). In this study, we examined the effects of ethylene signaling on root
337 hair initiation and ROS accumulation to determine if increased ethylene drives root hair initiation through
338 regulation of ROS producing enzymes and subsequent ROS accumulation in trichoblasts from which root
339 hairs form.

340 We examined root hair number and ROS accumulation in Col-0 treated with low concentrations
341 of ethylene gas (0.5 ppm) or the ethylene precursor, ACC (0.7 μM), for 4 hours. There was an increase in
342 the number of trichoblasts that formed root hairs in ethylene and ACC treated seedlings compared to
343 untreated controls, which was most pronounced in a 500 μm region starting 500 μm from the root tip, which
344 we call zone 2. Using a ratiometric reporter of ROS-induced gene expression, ZAT12p-ROS, we found that
345 in ACC-treated roots, ROS dependent gene expression was increased in zone 2 in ACC-treated roots
346 compared to untreated controls. We also examined the effect of ethylene and ACC on hydrogen peroxide
347 accumulation using a boronate based hydrogen peroxide selective sensor, PO1. Both ethylene and ACC
348 lead to elevated H_2O_2 accumulation in the trichoblast cells in zone 2 after 4 hours of treatment, but PO1
349 signal was at constant lower level in atrichoblast cells. There was a significant increase in PO1 signal within
350 2 hours after ACC treatment in cells that had not yet formed root hair bulges, suggesting that ethylene-
351 induced ROS acts to drive root hair initiation.

352 To examine whether canonical ethylene signaling controls ACC-dependent ROS synthesis driving
353 root hair formation, we examined these responses in several ethylene signaling mutants. In the ethylene
354 insensitive *ein3eill* and *etr1-3* mutants the effect of ACC treatment on ROS synthesis and root hair
355 formation is lost. In contrast, the *etr1-7* mutant allele that has constitutive signaling, has increased ROS and

356 root hair formation. These findings are consistent with our prior reports that showed that effects of this
357 ACC dose and under these growth conditions on root elongation, gravitropism, and lateral root formation
358 are lost in the ethylene insensitive *ein2-5* and *etr1-3* mutants (Harkey et al., 2018; Lewis et al., 2011; Negi
359 et al., 2010). These findings contrast with other processes in which higher doses of ACC can affect
360 development without conversion to ethylene, especially when the ACC oxidase enzyme is limited (Li et al.,
361 2021; Polko and Kieber, 2019; Van de Poel, 2020; Vanderstraeten et al., 2019). We also do not see ectopic
362 root hair formation in response to these short term and low dose treatments with ACC and ethylene, as
363 reported recently when seedlings were treated with 10ppm ethylene for 2 days (Qiu et al., 2021), which is
364 a 12-fold longer and 20-fold higher concentration.

365 If ROS is driving root hair formation, then it is predicted that mutants with impaired root hair
366 initiation, may have altered ROS levels. We examined the PO1 signal in the root hairless mutant, *caprice*
367 (*cpc*), and the *wereewolf* (*wer*) mutant that forms ectopic root hairs, both of which have mutations in MYB-
368 like DNA binding proteins (Lee and Schiefelbein, 1999; Wada et al., 1997). The *cpc* mutant showed a
369 significant decrease in PO1 signal when it is measured using line profiles along the root while *wer* showed
370 a significant increase, suggesting that mutants with altered root hair formation also show altered ROS
371 accumulation patterns. Similarly, the *rhd2-6* mutant, which was isolated for altered root hair elongation
372 (Foreman et al., 2003) and has impaired root hair formation (Gayomba and Muday, 2020) also had reduced
373 levels of ROS, suggesting a positive relationship between root hair formation and ROS levels using root
374 hair mutants.

375 Based on previous work detailing the role of RBOHC in root hair initiation and growth (Foreman
376 et al., 2003; Gayomba and Muday, 2020), we also asked whether this enzyme was contributing to ethylene-
377 induced ROS accumulation and subsequent root hair initiation and/or elongation. ACC treated *rhd2-6*,
378 which is an *RBOHC* null mutant, had a reduced number of root hairs, less root hair elongation, and
379 decreased ROS accumulation in trichoblasts compared to Col-0. We also saw more than a 2-fold increase
380 in RBOH activity in response to ACC treatment and a 3-fold reduction in activity in *rhd2-6* (*rboh*). These
381 data suggest that ethylene signaling induces ROS production in roots via increases in RBOHC enzyme
382 activity to drive root hair initiation and elongation but could also come from enhanced RBOHC synthesis.
383 We examined several transcriptomic datasets (Harkey et al., 2018; Harkey et al., 2019) and found evidence
384 of changes in *RBOHC* transcripts in response to ACC treatment, which were confirmed by qRT-PCR. The
385 ACC-induction was lost in the *ein3/eil1* mutant.

386 To determine if other root hair specific proteins and/or ROS producers are regulated by ethylene,
387 we widened our analysis of these previously published ACC and ethylene transcriptomic datasets. Although
388 ACC did not substantially change the abundance of transcripts encoding RHD2 (RBOHC), ROP2,

389 ROPGEF3, ROPGEF4, GL2, RHD6, or RSL4, we identified several transcripts that showed substantial
390 increase in response to ACC. Of particular interest were increases in transcripts encoding two class III
391 peroxidase enzymes PRX44 and PRX73, which showed a significant increase in abundance after 4 hours
392 of ACC treatment. ACC treatment of seedlings harboring a *pPRX44::GFP* construct lead to significant
393 increases in GFP fluorescence intensity in zone 2 compared to untreated controls, consistent with
394 transcriptional regulation of this gene. We also performed qRT-PCR and found a 2-fold increase in PRX44
395 transcripts in response to ACC treatment. Additionally, this ACC effect was lost in the *ein3/eil1* mutant and
396 that the abundance of *PRX44* transcripts was significantly lower in *ein3/eil1* even the absence of ACC
397 treatment.

398 ACC treatment of the null mutants *prx44-2* led to decreased ROS accumulation in root hair forming
399 trichoblasts, while there was no effect in *prx73-4* as compared to Col-0. The decreased PO1 signal in *prx44-*
400 2 was accompanied by significant reductions in the number of root hairs formed in this same root region
401 and the length of these root hairs. Together these experiments implicate RBOHC and Class III peroxidase
402 enzymes in ethylene-regulated ROS accumulation and root hair initiation.

403 These class III peroxidase enzymes have also been implicated as regulators of root hair growth in
404 response to environmental cues. Two PRXs are involved in auxin-dependent root hair elongation, as null
405 mutants treated with auxin have shorter root hairs and less ROS compared to wild type (Mangano et al.,
406 2017). Another report demonstrated that PRX enzymes function to modify the localization of extension
407 proteins to control cell wall structure to allow increased elongation (Marzol et al 2020). Recent work has
408 also indicated a role for PRXs as positive regulators of root hair growth at low temperatures (Pachecho et
409 al 2022). These results showed that low temperature induced root hair growth required peroxidase enzyme
410 activity and upregulated expression of PRXs that modulate ROS homeostasis and extensin stabilization to
411 drive root hair growth (Pachecho et al 2022). Prior publications and these results are consistent with a role
412 for peroxidases as drivers of root hair development and modulation of the apoplastic ROS pool.

413 To summarize our findings on ethylene-dependent root hair initiation via increased ROS synthesis
414 and to tie these findings with other studies, we present a model in Fig. 8. Low dose and short 4-hour
415 treatments with ACC led to efficient conversion of ACC to ethylene by roots to initiate an ethylene signaling
416 cascade. Ethylene acts through the ETR1 receptor and the canonical signaling pathway to increase the
417 activity of EIN3/EIL1 TFs. EIN3/EIL1 binds to the root hair specific TF RHD6 to induce RSL4 expression
418 and root hair elongation (Feng et al., 2017). Root hair growth is controlled by several proteins leading to
419 activation of the RHD6 TF. Downstream of RHD6, the RSL4 TF acts to define final root hair length based
420 on its level of expression (Datta et al., 2015; Mangano et al., 2017). Previous work has shown that EIN3
421 physically interacts with RHD6 to form a transcriptional complex that coactivate RSL4 to promote root

422 hair elongation (Feng et al., 2017), and that EIN3 and RSL4 both act to downregulate GL2 expression to
423 drive ectopic root hair formation with long term treatments with high levels of ethylene (Qiu et al., 2021).
424 It has also been shown that auxin treatment results in increased RSL4 transcript abundance, which binds to
425 the promoters of RBOH and four class III peroxidase (*PRX*) genes, including *PRX44*, to drive ROS
426 synthesis in root hair cells. RSL4 activation via auxin induces class III peroxidase and *RBOH* expression,
427 which leads to ROS accumulation required to drive root hair elongation (Mangano et al., 2017). We find
428 that ACC treatment increases activity of RBOHC enzymes leading to increased ROS and root hair
429 elongation, without changing the abundance of *RBOHC* transcripts. Additionally, ACC treatment leads to
430 the transcriptional regulation of class III peroxidases and RBOHC, resulting in ROS production and root
431 hair initiation. Although the reduction in ROS in *rhd2-6* and *prx44-2*, in both the presence absence of ACC
432 was expected, we did not expect that there would still be an increase in root hair number in response to
433 ACC. This data suggests that perhaps the ROS selective dyes that we have access to are not sensitive enough
434 to detect the small changes in ROS that occur prior to root hair initiation in these mutants or that there are
435 additional mechanisms that may facilitate ethylene-induced root hair formation, including redundant action
436 of these two enzymes. Further investigation regarding the mechanisms of ethylene-regulated ROS synthesis
437 is required. For example, one important question to be answered is how ethylene signaling regulates RBOH
438 activity. This could occur through a number of different mechanisms, such as calcium binding or
439 phosphorylation, which are known to regulate RBOH enzymes (Postiglione and Muday, 2020).

440 This work supports the role of ROS as a signaling molecule, in which ROS are produced in response
441 to hormonal cues to drive developmental processes. We provide new evidence for the ethylene regulation
442 of the ROS producing enzymes, RBOHC and class III PRX44. However, there are other ROS producing
443 and scavenging enzymes, such as superoxide dismutase (SODs), that require additional study to understand
444 the numerous developmental mechanisms that ROS may play a role in. It is also crucial to understand the
445 molecular mechanisms by which ROS regulates the activity of proteins that drive root hair initiation and
446 elongation. ROS can oxidize cysteine residues in proteins to change their conformation and activity
447 (Couturier et al., 2013) so a critical next step is to identify those root hair proteins are modified by ROS to
448 drive this important developmental process.

449

450 MATERIALS AND METHODS

451 Growth conditions and root hair quantification

452 All Arabidopsis mutants were in the Col-0 background. The *etr1-7*, *etr1-3* (AT1G66340), *ein3-1*
453 (AT3G20770) *eil1-1* (AT2G27050) double and *rhd2-6* (AT5G51060) mutants have all been described
454 previously (Binder et al., 2007; Gayomba and Muday, 2020; Harkey et al., 2018; Hua and Meyerowitz,
455 1998). The ZAT12p-ROS construct was generously provided by Won-Gyu Choi (Lim et al., 2019). *prx44-*
456 *2* (AT4G06010) and *prx73-4* (AT5G67400) were obtained from the Arabidopsis SALK center
457 (SALK_057222C and SALK_020724, respectively), the mutations were verified by PCR, and homozygous
458 lines were isolated. The transcriptional reporter *pPRX44::GFP* transgenic line was described previously
459 (Marzol, 2021). Seeds were sterilized in 75% ethanol for approximately 5 minutes and grown on 100 x 15
460 mm Petri dishes containing 25 mL media. Seedlings were grown on 1x MS supplemented with 1% sucrose,
461 vitamins (1 µg/ml thiamine, 0.5 µg/ml pyridoxine and 0.5 µg/ml nicotinic acid), 0.05% MES (w/v) and
462 0.8% (w/v) agar. Media pH was 5.5. Micropore tape was used to seal the top of the Petri dish and plated
463 seeds were stratified at 4° C in darkness for 2 days. Plants were grown under 24h light from T5 fluorescent
464 lights at 120-150 µmol photons m⁻² s⁻¹.

465 ACC and ethylene treatments

466 ACC stocks at 200 mM were prepared using ACC hydrochloride diluted in H₂O. ACC was then added
467 directly to media to yield of final concentration of 0.7 µM. Seeds were grown on control plates as described
468 above for 5 days and then transferred to plates containing either 0.7 µM of ACC or transferred to new plates
469 and placed in an air tight tank containing 0.5 ppm ethylene gas. Seedlings were then left under the light
470 conditions described above for 4 hours and then used for experiments.

471 Quantification of root hair number and root hair length

472 Seedlings were grown for 5 days on control media and then transferred to media containing 0.7 µM
473 ACC and grown for 4 hours or other indicated times. To examine root hairs, 5-day old seedlings were
474 imaged using bright-field on an Axio Zoom V16 stereomicroscope. Extended depth of focus was used to
475 combine z-stack images. Root hairs that were at stage +1 or +2 (or later stages) as defined by (Denninger
476 et al., 2019) were quantified using Fiji/ImageJ software in three zones (0-500 µm, 500-1000 µm, 1000-1500
477 µm) starting from the root tip.

478 We also determined root hair length in the presence and absence of ACC treatment in Col-0 ad
479 mutants. All root hairs in zone 2 that had begun to elongate (were at stages above +2) were measured using
480 Fiji/ImageJ software. The length of each root in microns was determined. To obtain the histogram of

481 distribution, the roots were separated into bins of different lengths, and the % of root hairs in each length
482 bin was determined by dividing by the total number of root hairs in Zone 2 in that root.

483 **Confocal imaging of dyes and reporters of ROS levels**

484 H_2O_2 was visualized with Peroxy-Orange 1 (PO1). PO1 was dissolved in DMSO to make a 500
485 μM stock and was further diluted in H_2O to make a 50 μM working solution. Seedlings were incubated in
486 PO1 for 15 minutes in the dark and were then rinsed with H_2O and mounted in H_2O for imaging. Control,
487 ACC-treated and ethylene-treated seedlings were imaged on a Zeiss 880 laser scanning confocal
488 microscope using a 10x objective. PO1 was excited with a 488 nm laser at 0.25% power and emission was
489 collected between 544-695 nm. Images were analyzed using Fiji/ImageJ software. Plot profiles were taken
490 across the epidermal cell files of maximum intensity projections using a 20-pixel line and values were
491 averaged within each cell file. All images were captured at levels below saturation, although images shown
492 in the manuscript were uniformly adjusted for brightness and contrast for clarity.

493 5-day old seedlings harboring the ZAT12p-ROS construct were mounted in H_2O and excited with
494 488 and 561 nm lasers at 6% and 1.2% laser power, respectively. GFP emission was collected at 521 nm
495 and mCherry emission was collected at 593 nm. Fiji/ImageJ software was used to generate two single
496 channel images to form individual GFP and mCherry channels. Plot profiles were taken using a 250-pixel
497 wide line to measure fluorescence of the entire root. Measurements were taken starting at 200 μm back
498 from the root tip and ending at 1500 μm . Ratios were generated by dividing the GFP channel by mCherry
499 using the Image Calculator tool (Process/Image Calculator).

500 **PI staining and *proPRX44::GFP* imaging**

501 Cell walls were stained with 0.5 $\mu\text{g}/\text{mL}$ propidium iodide (PI) dissolved in H_2O . 5 day old seedlings
502 treated with and without ACC were incubated in PI for 4 minutes before imaging. Fluorescence was
503 visualized using a 561 nm laser at 0.15% and emission spectra set to 561-695 nm. These settings were used
504 for all images. Optical slices of the top section of the root to show epidermal cells and maximum intensity
505 projections of z-stack images are shown in Fig. S1. Fiji software was used to measure cell length of 3
506 epidermal cells per root using optical slices of the top section of the root. Cells were chosen at the bottom
507 of zone 2 (cell 1, in the middle (cell 2), and at the top (cell 3). 4 cells of each of the 3 cell types were
508 averaged and are shown in FS1. 6-8 roots of both control and ACC treated seedlings. Transgenic seeds
509 harboring *pPRX44::GFP* were obtained from the lab of Dr. Jose Estevez, 5-day old seedlings were mounted
510 in H_2O and excited with a 488 nm laser at 5% and emission was collected between 490-606 nm. Seedlings
511 were then stained with PI.

512 **DNA extraction and PCR for mutant genotype analysis**

513 T-DNA insertion lines were grown for approximately 2 weeks on media described above, then
514 transferred to soil and grown under 24h light at 50-80 $\mu\text{mol photons m}^{-2} \text{s}^{-1}$. Leaves were harvested from 6
515 week old plants and stored in eppendorf tubes at -20°C prior to DNA extraction. Frozen leaves were ground
516 in DNA extraction buffer (100 mM Tris-HCl pH 8.0, 10 mM Na₂EDTA, 100 mM LiCl₂, 1% (w/v) SDS).
517 Samples were then washed once with isopropanol and three times with 80% (v/v) ethanol. Finally, DNA
518 pellets were dried, resuspended in sterile H₂O and stored at -20°C . Each PCR reaction contained 1X GoTaq
519 Polymerase, 1 μM of each primer, 1 μL of DNA and 5 μL H₂O. To confirm that mutants were homozygous
520 for the desired T-DNA insertion, one reaction was performed with primers (left primer and right primer)
521 flanking the left and right sides of in-tact genes while one reaction was performed with the right primer and
522 LBb1.3, which is a primer specific for the left border of the T-DNA insertion. PCR products were run on
523 0.8 % (w/v) agarose gels containing 0.002% SERVA DNA stain G.

524 **RNA Isolation and Quantitative Real Time-PCR**

525 RNA was isolated from seedlings grown on a nylon filter as described previously (Harkey et al., 2018). 5-
526 days after germination seedlings were transferred to either control media or media containing 0.7 μM ACC
527 and were grown for 4 hours. Roots were then cut and flash frozen in liquid nitrogen then ground. RNA was
528 isolated using the Qiagen plant RNeasy kit protocol and RNA was DNase treated.

529 cDNA synthesis was performed using the RevertAid RT Reverse Transcription kit (ThermoFisher). qRT-
530 PCR analysis using this cDNA was performed on a QuantStudio real time PCR machine using SYBR green
531 detection chemistry. Primers specific to *PRX44* (FP: 5'-CAA GAG ACT CGG TCG CAT TAG-3' and RP:
532 5'-TTG TTG GTC CGG GTA AGT TC-3') and *RBOHC* (FP: 5'-CAA GGA ACA AGC CCA ACT AAA-
533 3' and RP: 5'-TTC TAT TGG GTT ACG CGT GAG-3') were used and relative transcript abundance was
534 quantified using ACT2 primers using comparative Ct analysis ($\Delta\Delta\text{Ct}$) to determine the relative quantity of
535 target transcripts.

536 **NADPH oxidase/RBOH enzyme assays**

537 Protein extract was isolated from seedlings grown on a nylon filter as described previously (Harkey
538 et al., 2018). After 2 days of stratification and 7 days of growth under conditions described above, the nylon
539 was transferred to growth medium with and without 0.7 μM ACC for 4 hours. Roots were then cut from
540 seedlings and flash frozen in liquid nitrogen. Frozen samples were ground in liquid nitrogen using a mortar
541 and pestle. RBOH extraction buffer (50 mM Tris-HCl pH 7.5, 0.1 mM EDTA, 0.1% (v/v) Triton X-100, 1
542 mM MgCl₂, 10% (v/v) glycerol) was then added to a plant material/buffer ratio of 1:3 (w/v). Samples were

543 centrifuged and supernatant was collected and desalted and concentrated using the Amicon Ultra-0.5
544 Centrifugal Filter devices. RBOH reaction mixture (50 mM Tris-HCl pH 7.5, 1 mM CaCl₂, 0.1 mM
545 nitroblue tetrazolium (NBT), 0.1 mM NADPH) was then mixed with protein extract at a 1:1 ratio. The
546 reduction of NBT to monoformazan was monitored spectrophotometrically at 530 nm. Monoformazan
547 concentrations were calculated using a 12.8 mM⁻¹cm⁻¹ extinction coefficient. This assay was adapted in
548 sweet peppers and has previously been described (Chu-Puga et al., 2019).

549 **ACKNOWLEDGMENTS**

550 We would like to thank Dr. Brad Binder (University of Tennessee) and all Muday lab members for their
551 editorial input, and Dr. Glen Marrs and Dr. Heather Brown-Harding (Wake Forest University) for their help
552 with microscopy.

553 **COMPETING INTERESTS**

554 The authors have no competing interests.

555 **FUNDING**

556 This project was supported by the National Science Foundation (MCB-1716279 to GKM) and a USDA
557 Predoctoral Fellowship (NIFA 2021-67034-35113 to REM). Dr. Jose Estevez and Dr. Eliana Marzol are
558 investigators of the National Research Council (CONICET) from Argentina supported by grants from
559 ANPCyT (PICT2019-0015 to J.M.E. and PICT2018-0577 to E.M.) and ANID – Programa Iniciativa
560 Científica Milenio ICN17_022, NCN2021_010 and Fondo Nacional de Desarrollo Científico y Tecnológico
561 [1200010] to J.M.E.

562 **DATA AVAILABILITY**

563 All data in this manuscript are included in the text or in the supplementary file.

564 **Reference List**

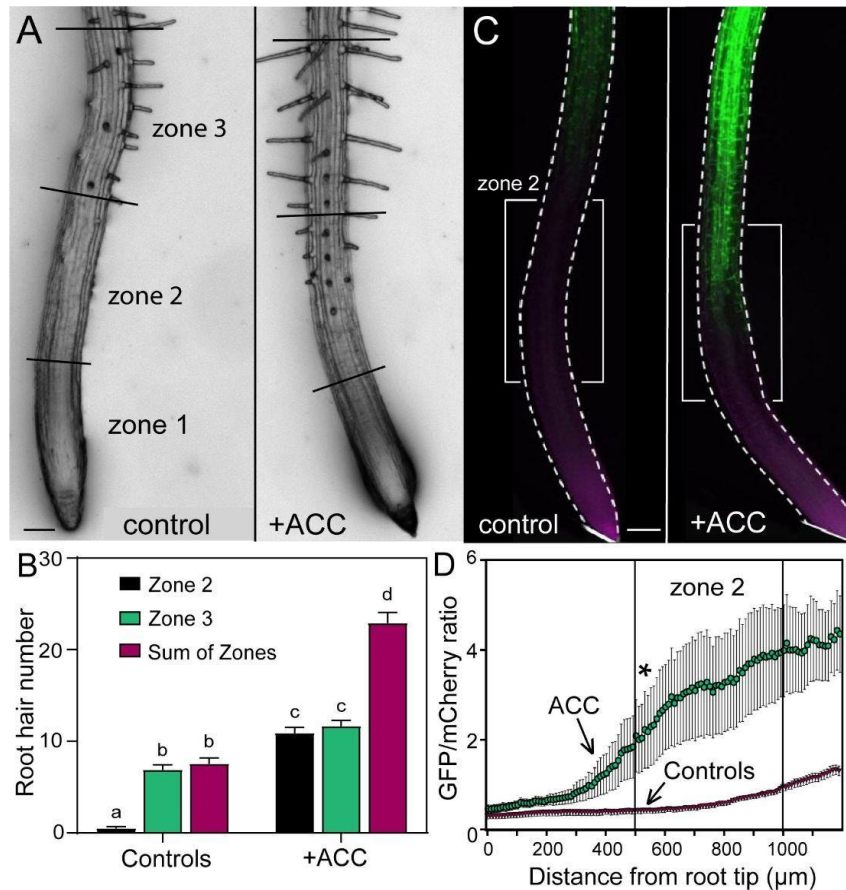
- 565 **Alonso, J. M., Hirayama, T., Roman, G., Nourizadeh, S. and Ecker, J. R.** (1999). EIN2, a bifunctional
566 transducer of ethylene and stress responses in Arabidopsis. *Science* **284**, 2148-2152.
- 567 **Berger, F., Haseloff, J., Schiefelbein, J. and Dolan, L.** (1998). Positional information in root epidermis
568 is defined during embryogenesis and acts in domains with strict boundaries. *Curr Biol* **8**, 421-430.
- 569 **Bienert, G. P., Moller, A. L. B., Kristiansen, K. A., Schulz, A., Moller, I. M., Schjoerring, J. K. and**
570 **Jahn, T. P.** (2007). Specific aquaporins facilitate the diffusion of hydrogen peroxide across
571 membranes. *J Biol Chem* **282**, 1183-1192.
- 572 **Binder, B. M.** (2020). Ethylene signaling in plants. *J Biol Chem* **295**, 7710-7725.
- 573 **Binder, B. M., Walker, J. M., Gagne, J. M., Emborg, T. J., Hemmann, G., Bleecker, A. B. and**
574 **Vierstra, R. D.** (2007). The Arabidopsis EIN3 binding F-box proteins EBF1 and EBF2 have
575 distinct but overlapping roles in ethylene signaling. *Plant Cell* **19**, 509-523.
- 576 **Bleecker, A. B.** (1999). Ethylene perception and signaling: an evolutionary perspective. *Trends Plant Sci*
577 **4**, 269-274.
- 578 **Bruex, A., Kainkaryam, R. M., Wieckowski, Y., Kang, Y. H., Bernhardt, C., Xia, Y., Zheng, X.,**
579 **Wang, J. Y., Lee, M. M., Benfey, P., et al.** (2012). A gene regulatory network for root epidermis
580 cell differentiation in Arabidopsis. *Plos Genet* **8**, e1002446.
- 581 **Carroll, A. D., Moyon, C., Van Kesteren, P., Tooke, F., Battey, N. H. and Brownlee, C.** (1998). Ca²⁺,
582 annexins, and GTP modulate exocytosis from maize root cap protoplasts. *Plant Cell* **10**, 1267-1276.
- 583 **Chao, Q. M., Rothenberg, M., Solano, R., Roman, G., Terzaghi, W. and Ecker, J. R.** (1997). Activation
584 of the ethylene gas response pathway in Arabidopsis by the nuclear protein ETHYLENE-
585 INSENSITIVE3 and related proteins. *Cell* **89**, 1133-1144.
- 586 **Chapman, J. M., Muhlemann, J. K., Gayomba, S. R. and Muday, G. K.** (2019). RBOH-Dependent
587 ROS Synthesis and ROS Scavenging by Plant Specialized Metabolites To Modulate Plant
588 Development and Stress Responses. *Chem Res Toxicol* **32**, 370-396.
- 589 **Chu-Puga, A., Gonzalez-Gordo, S., Rodriguez-Ruiz, M., Palma, J. M. and Corpas, F. J.** (2019).
590 NADPH Oxidase (Rboh) Activity is Up Regulated during Sweet Pepper (*Capsicum annuum* L.)
591 Fruit Ripening. *Antioxidants-Basel* **8**, 9.
- 592 **Couturier, J., Chibani, K., Jacquot, J. P. and Rouhier, N.** (2013). Cysteine-based redox regulation and
593 signaling in plants. *Front Plant Sci* **4**, 105.
- 594 **Datta, S., Prescott, H. and Dolan, L.** (2015). Intensity of a pulse of RSL4 transcription factor synthesis
595 determines Arabidopsis root hair cell size. *Nat Plants* **1**:15138.
- 596 **De Baets, S., Denbigh, T. D. G., Smyth, K. M., Eldridge, B. M., Weldon, L., Higgins, B.,**
597 **Matyjaszkiewicz, A., Meersmans, J., Larson, E. R., Chenchiah, I. V., et al.** (2020). Micro-scale
598 interactions between Arabidopsis root hairs and soil particles influence soil erosion. *Commun Biol*
599 **3** (1), 164.
- 600 **Denninger, P., Reichelt, A., Schmidt, V. A. F., Mehlhorn, D. G., Asseck, L. Y., Stanley, C. E., Keinath,**
601 **N. F., Evers, J. F., Grefen, C. and Grossmann, G.** (2019). Distinct RopGEFs Successively Drive
602 Polarization and Outgrowth of Root Hairs. *Curr Biol* **29**, 1854-+.
- 603 **Di Cristina, M., Sessa, G., Dolan, L., Linstead, P., Baima, S., Ruberti, I. and Morelli, G.** (1996). The
604 Arabidopsis Athb-10 (GLABRA2) is an HD-Zip protein required for regulation of root hair
605 development. *Plant J* **10**, 393-402.
- 606 **Dickinson, B. C., Huynh, C. and Chang, C. J.** (2010). A Palette of Fluorescent Probes with Varying
607 Emission Colors for Imaging Hydrogen Peroxide Signaling in Living Cells. *J Am Chem Soc* **132**,
608 5906-5915.
- 609 **Dolan, L., Duckett, C. M., Grierson, C., Linstead, P., Schneider, K., Lawson, E., Dean, C., Poethig,**
610 **S. and Roberts, K.** (1994). Clonal Relationships and Cell Patterning in the Root Epidermis of
611 Arabidopsis. *Development* **120**, 2465-2474.

- 612 **Feng, Y., Xu, P., Li, B., Li, P., Wen, X., An, F., Gong, Y., Xin, Y., Zhu, Z., Wang, Y., et al.** (2017).
613 Ethylene promotes root hair growth through coordinated EIN3/EIL1 and RHD6/RSL1 activity in
614 Arabidopsis. *Proc Natl Acad Sci U S A* **114**, 13834-13839.
- 615 **Foreman, J., Demidchik, V., Bothwell, J. H., Mylona, P., Miedema, H., Torres, M. A., Linstead, P.,**
616 **Costa, S., Brownlee, C., Jones, J. D., et al.** (2003). Reactive oxygen species produced by NADPH
617 oxidase regulate plant cell growth. *Nature* **422**, 442-446.
- 618 **Galway, M. E., Masucci, J. D., Lloyd, A. M., Walbot, V., Davis, R. W. and Schiefelbein, J. W.** (1994).
619 The Ttg Gene Is Required to Specify Epidermal-Cell Fate and Cell Patterning in the Arabidopsis
620 Root. *Dev Biol* **166**, 740-754.
- 621 **Gayomba, S. R. and Muday, G. K.** (2020). Flavonols regulate root hair development by modulating
622 accumulation of reactive oxygen species in the root epidermis. *Development* **147**, dev185819.
- 623 **Grebe, M.** (2012). The patterning of epidermal hairs in Arabidopsis - updated. *Curr Opin Plant Biol* **15**,
624 31-37.
- 625 **Guzman, P. and Ecker, J. R.** (1990). Exploiting the triple response of Arabidopsis to identify ethylene-
626 related mutants. *Plant Cell* **2**, 513-523.
- 627 **Harkey, A. F., Watkins, J. M., Olex, A. L., DiNapoli, K. T., Lewis, D. R., Fetrow, J. S., Binder, B. M.**
628 **and Muday, G. K.** (2018). Identification of Transcriptional and Receptor Networks That Control
629 Root Responses to Ethylene. *Plant Physiol* **176**, 2095-2118.
- 630 **Harkey, A. F., Yoon, G. M., Seo, D. H., DeLong, A. and Muday, G. K.** (2019). Light Modulates Ethylene
631 Synthesis, Signaling, and Downstream Transcriptional Networks to Control Plant Development.
632 *Front Plant Sci* **10**.
- 633 **Hua, J. and Meyerowitz, E. M.** (1998). Ethylene responses are negatively regulated by a receptor gene
634 family in Arabidopsis thaliana. *Cell* **94**, 261-271.
- 635 **Jones, M. A., Raymond, M. J., Yang, Z. B. and Smirnov, N.** (2007). NADPH oxidase-dependent reactive
636 oxygen species formation required for root hair growth depends on ROP GTPase. *J Exp Bot* **58**,
637 1261-1270.
- 638 **Ju, C., Yoon, G. M., Shemansky, J. M., Lin, D. Y., Ying, Z. I., Chang, J., Garrett, W. M., Kessenbrock,**
639 **M., Groth, G., Tucker, M. L., et al.** (2012). CTR1 phosphorylates the central regulator EIN2 to
640 control ethylene hormone signaling from the ER membrane to the nucleus in Arabidopsis. *Proc*
641 *Natl Acad Sci U S A* **109**, 19486-19491.
- 642 **Kieber, J. J., Rothenberg, M., Roman, G., Feldmann, K. A. and Ecker, J. R.** (1993). Ctr1, a Negative
643 Regulator of the Ethylene Response Pathway in Arabidopsis, Encodes a Member of the Raf Family
644 of Protein-Kinases. *Cell* **72**, 427-441.
- 645 **Kobayashi, M., Ohura, I., Kawakita, K., Yokota, N., Fujiwara, M., Shimamoto, K., Doke, N. and**
646 **Yoshioka, H.** (2007). Calcium-dependent protein kinases regulate the production of reactive
647 oxygen species by potato NADPH oxidase. *Plant Cell* **19**, 1065-1080.
- 648 **Kwak, J. M., Mori, I. C., Pei, Z. M., Leonhardt, N., Torres, M. A., Dangel, J. L., Bloom, R. E., Bodde,**
649 **S., Jones, J. D. and Schroeder, J. I.** (2003). NADPH oxidase AtrbohD and AtrbohF genes
650 function in ROS-dependent ABA signaling in Arabidopsis. *EMBO J* **22**, 2623-2633.
- 651 **Leavitt, R.** (1904). Trichomes of the root of vascular cryptogams and angiosperms. *Proceedings of the*
652 *Boston Society of Natural History* **31**, 273-313.
- 653 **Lee, M. M. and Schiefelbein, J.** (1999). WEREWOLF, a MYB-related protein in Arabidopsis, is a
654 position-dependent regulator of epidermal cell patterning. *Cell* **99**, 473-483.
- 655 **Lewis, D. R., Negi, S., Sukumar, P. and Muday, G. K.** (2011). Ethylene inhibits lateral root development,
656 increases IAA transport and expression of PIN3 and PIN7 auxin efflux carriers. *Development* **138**,
657 3485-3495.
- 658 **Li, D., Mou, W., Van de Poel, B. and Chang, C.** (2021). Something old, something new: Conservation of
659 the ethylene precursor 1-amino-cyclopropane-1-carboxylic acid as a signaling molecule. *Curr Opin*
660 *Plant Biol* **65**, 102116.

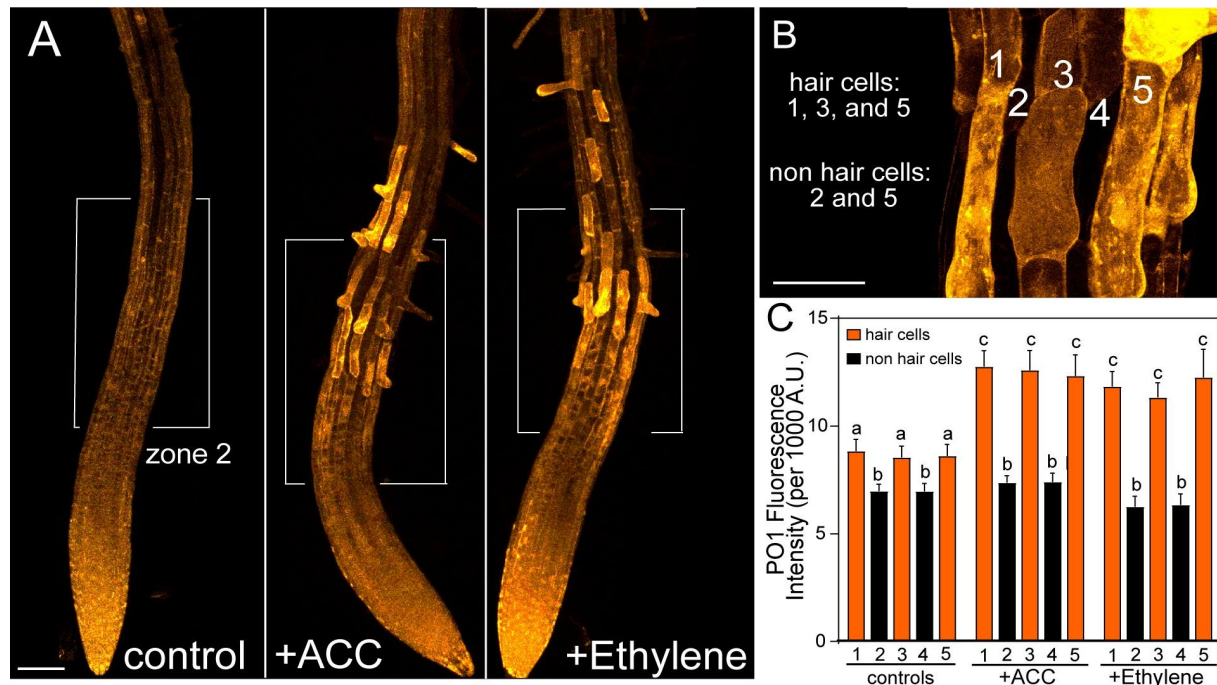
- 661 **Lim, S. D., Kim, S. H., Gilroy, S., Cushman, J. C. and Choi, W. G.** (2019). Quantitative ROS
662 bioreporters: A robust toolkit for studying biological roles of ROS in response to abiotic and biotic
663 stresses. *Physiol Plantarum* **165**, 356-368.
- 664 **Mangano, S., Denita-Juarez, S. P., Choi, H. S., Marzol, E., Hwang, Y., Ranocha, P., Velasquez, S. M.,**
665 **Borassi, C., Barberini, M. L., Aptekmann, A. A., et al.** (2017). Molecular link between auxin
666 and ROS-mediated polar growth. *P Natl Acad Sci USA* **114**, 5289-5294.
- 667 **Marzol, E., Borassi, C., Ranocha, P., Aptekman, A.A., Bringas, M., Pennington, J., Paez-Valencia, J.,**
668 **Pacheco, J.M., Garcia, D.R.R., Guerrero, Y.D.C, Carignani, M., Mangano, S., Fleming, M.,**
669 **Mishler-Elmore, J.W., Blanco-Herrera, F., Bedinger, P., Dunand, C., Capece, L., Nadra,**
670 **A.D., Held, M., Otegu, M., Estevez, J.M** (2021). Class III peroxidases PRX01, PRX44, and
671 PRX73 potentially target extensins during root hair growth in *Arabidopsis thaliana*. *bioRxiv*
672 **Preprint**.
- 673 **Masucci, J. D. and Schiefelbein, J. W.** (1994). The Rhd6 Mutation of *Arabidopsis-Thaliana* Alters Root-
674 Hair Initiation through an Auxin-Associated and Ethylene-Associated Process. *Plant Physiol* **106**,
675 1335-1346.
- 676 **Masucci, J. D. and Schiefelbein, J. W.** (1996). Hormones act downstream of TTG and GL2 to promote
677 root hair outgrowth during epidermis development in the *Arabidopsis* root. *Plant Cell* **8**, 1505-
678 1517.
- 679 **Mittler, R., Vanderauwera, S., Suzuki, N., Miller, G., Tognetti, V. B., Vandepoele, K., Gollery, M.,**
680 **Shulaev, V. and Van Breusegem, F.** (2011). ROS signaling: the new wave? *Trends Plant Sci* **16**,
681 300-309.
- 682 **Molendijk, A. J., Bischoff, F., Rajendrakumar, C. S. V., Friml, J., Braun, M., Gilroy, S. and Palme,**
683 **K.** (2001). *Arabidopsis thaliana* Rop GTPases are localized to tips of root hairs and control polar
684 growth. *Embo J* **20**, 2779-2788.
- 685 **Monshausen, G. B., Bibikova, T. N., Messerli, M. A., Shi, C. and Gilroy, S.** (2007). Oscillations in
686 extracellular pH and reactive oxygen species modulate tip growth of *Arabidopsis* root haris. *P Natl*
687 *Acad Sci USA* **104**, 20996-21001.
- 688 **Negi, S., Sukumar, P., Liu, X., Cohen, J. D. and Muday, G. K.** (2010). Genetic dissection of the role of
689 ethylene in regulating auxin-dependent lateral and adventitious root formation in tomato. *Plant J*
690 **61**, 3-15.
- 691 **Pemberton, L. M. S., Tsai, S. L., Lovell, P. H. and Harris, P. J.** (2001). Epidermal patterning in seedling
692 roots of eudicotyledons. *Ann Bot-London* **87**, 649-654.
- 693 **Polko, J. K. and Kieber, J. J.** (2019). 1-Aminocyclopropane 1-Carboxylic Acid and Its Emerging Role as
694 an Ethylene-Independent Growth Regulator. *Front Plant Sci* **10**, 1602.
- 695 **Poole, L. B. and Schoneich, C.** (2015). Introduction: What we do and do not know regarding redox
696 processes of thiols in signaling pathways. *Free Radical Bio Med* **80**, 145-147.
- 697 **Postiglione, A. E. and Muday, G. K.** (2020). The Role of ROS Homeostasis in ABA-Induced Guard Cell
698 Signaling. *Front Plant Sci* **11**.
- 699 **Qiu, Y., Tao, R., Feng, Y., Xiao, Z., Zhang, D., Peng, Y., Wen, X., Wang, Y. and Guo, H.** (2021). EIN3
700 and RSL4 interfere with an MYB-bHLH-WD40 complex to mediate ethylene-induced ectopic root
701 hair formation in *Arabidopsis*. *Proc Natl Acad Sci U S A* **118**.
- 702 **Rerie, W. G., Feldmann, K. A. and Marks, M. D.** (1994). The *Glabra2* Gene Encodes a Homeo Domain
703 Protein Required for Normal Trichome Development in *Arabidopsis*. *Gene Dev* **8**, 1388-1399.
- 704 **Salazar-Henao, J. E., Velez-Bermudez, I. C. and Schmidt, W.** (2016). The regulation and plasticity of
705 root hair patterning and morphogenesis. *Development* **143**, 1848-1858.
- 706 **Schiefelbein, J., Huang, L. and Zheng, X. H.** (2014). Regulation of epidermal cell fate in *Arabidopsis*
707 roots: the importance of multiple feedback loops. *Front Plant Sci* **5**.
- 708 **Schiefelbein, J. W. and Somerville, C.** (1990). Genetic-Control of Root Hair Development in *Arabidopsis-*
709 *Thaliana*. *Plant Cell* **2**, 235-243.
- 710 **Shibata, M. and Sugimoto, K.** (2019). A gene regulatory network for root hair development. *J Plant Res*
711 **132**, 301-309.

- 712 **Solano, R., Stepanova, A., Chao, Q. and Ecker, J. R.** (1998). Nuclear events in ethylene signaling: a
713 transcriptional cascade mediated by ETHYLENE-INSENSITIVE3 and ETHYLENE-RESPONSE-
714 FACTOR1. *Genes Dev* **12**, 3703-3714.
- 715 **Suzuki, N., Miller, G., Morales, J., Shulaev, V., Torres, M. A. and Mittler, R.** (2011). Respiratory burst
716 oxidases: the engines of ROS signaling. *Curr Opin Plant Biol* **14**, 691-699.
- 717 **Takeda, S., Gapper, C., Kaya, H., Bell, E., Kuchitsu, K. and Dolan, L.** (2008). Local positive feedback
718 regulation determines cell shape in root hair cells. *Science* **319**, 1241-1244.
- 719 **Tanimoto, M., Roberts, K. and Dolan, L.** (1995). Ethylene is a positive regulator of root hair development
720 in *Arabidopsis thaliana*. *Plant J* **8**, 943-948.
- 721 **Van de Poel, B.** (2020). Ethylene's fraternal twin steals the spotlight. *Nat Plants* **6**, 1309-1310.
- 722 **Vanderstraeten, L., Depaepe, T., Bertrand, S. and Van Der Straeten, D.** (2019). The Ethylene Precursor
723 ACC Affects Early Vegetative Development Independently of Ethylene Signaling. *Front Plant Sci*
724 **10**, 1591.
- 725 **Wada, T., Tachibana, T., Shimura, Y. and Okada, K.** (1997). Epidermal cell differentiation in
726 *Arabidopsis* determined by a Myb homolog, CPC. *Science* **277**, 1113-1116.
- 727 **Wen, X., Zhang, C., Ji, Y., Zhao, Q., He, W., An, F., Jiang, L. and Guo, H.** (2012). Activation of
728 ethylene signaling is mediated by nuclear translocation of the cleaved EIN2 carboxyl terminus. *Cell*
729 *Res* **22**, 1613-1616.

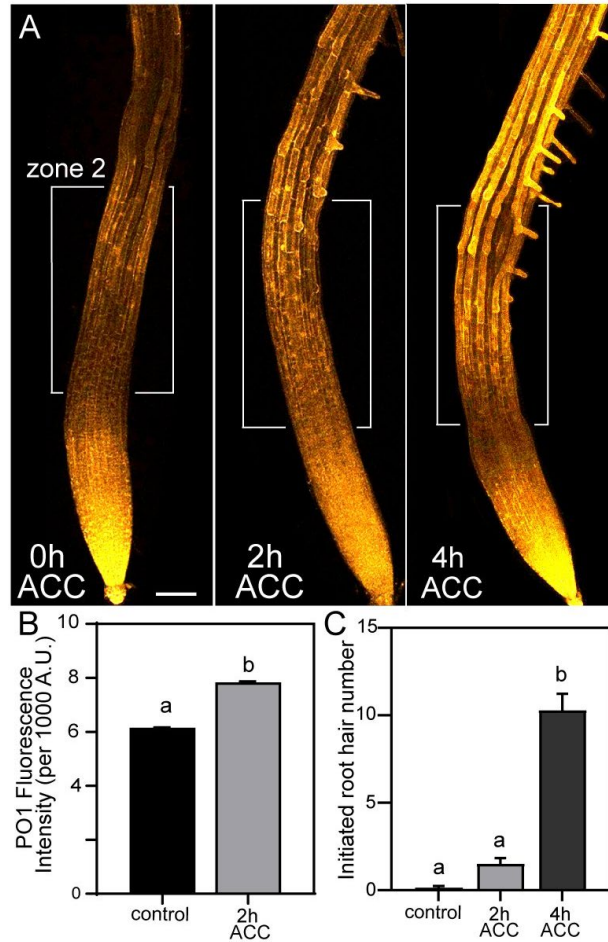
730



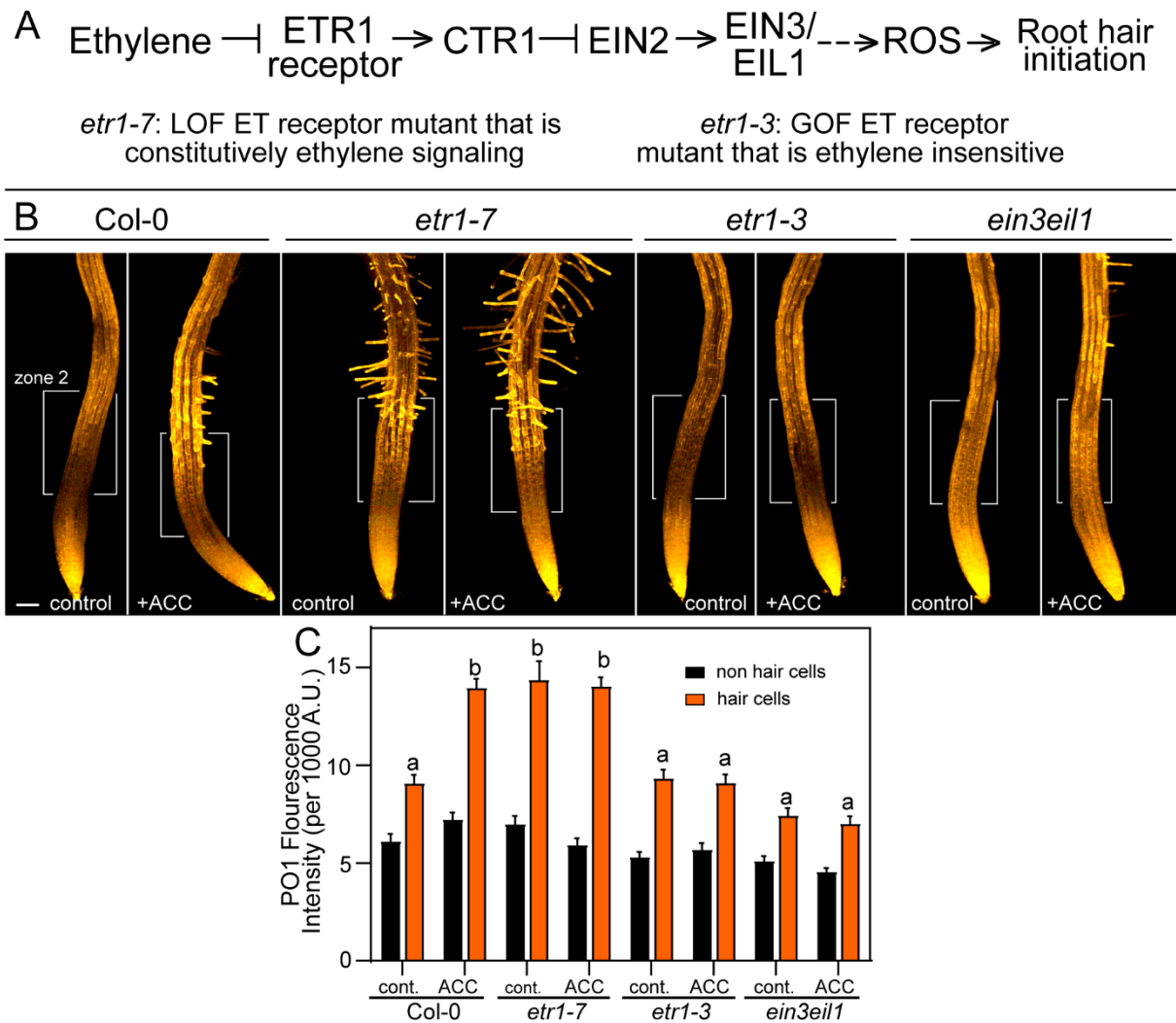
731 **Figure 1. ACC treatment increases root hair number and ROS dependent gene expression along the**
732 **root after 4 hours** (A) Representative images of root tips of Col-0 treated with and without ACC for 4
733 hours. Zones 1, 2, and 3 represent 500 μm root sections. Scale bar for all images are 100 μm . (B) Root
734 hair quantification of untreated and 4h ACC treated seedlings. No root hairs formed in zone 1. Data are
735 means \pm SEM of total RH in zone 2, zone 3, and all zones from 3 experiments (n=18-24 seedlings per
736 experiment). Columns with different letters indicate statistically significant differences determined by
737 two-way ANOVA followed by Tukey's multiple comparisons test. (C) Representative images of root tips
738 of Col-0 containing the ZAT12p-ROS reporter treated with or without ACC for 4 hours with GFP signal
739 in green and mCherry signal in magenta. White brackets indicate zone 2 of the root. (D) Quantification
740 of the ratio of GFP/mCherry fluorescence intensity using a line profile along the roots of an average of 6-12
741 seedlings of 3 independent experiments of untreated or ACC treated seedlings. Data are means \pm SEM.
742 The asterisk represents the shortest distance from the root tip at which the GFP fluorescence in the
743 presence of ACC values became significantly different from the controls as determined by student's t-test
744 (at approximately 510 μm).



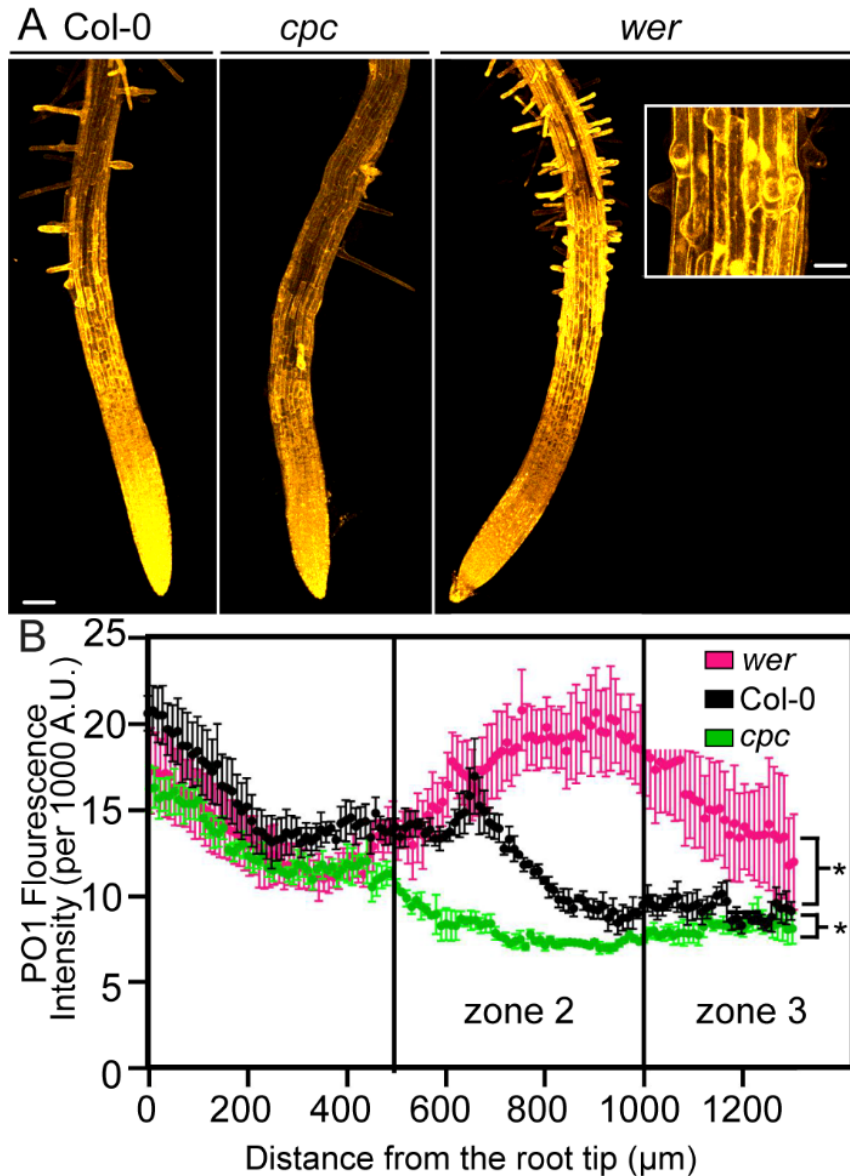
745 **Figure 2. ACC and ethylene gas increase H₂O₂ accumulation in trichoblasts after 4 hours.** (A)
 746 Representative roots illustrating the alternating PO1 fluorescence between trichoblast and atrichoblast
 747 epidermal cell files of cells in Col-0 roots with and without ACC and ethylene gas treatment for 4 hours.
 748 White brackets indicate zone 2 of the root. Scale bar is 100 μm. (B) Inset of hair cells (1, 3, 5) vs. non
 749 hair cells (2, 4) from roots treated with ethylene. Scale bar is 50 μm. (C) Quantification of PO1
 750 fluorescence intensity in trichoblasts (orange bars: 1, 3 and 5) and atrichoblasts (black bars: 2, 4). Data are
 751 the means ± SEM of 3 independent experiments (n=18-24 seedlings/experiment). Columns with different
 752 letters indicate statistical significance compared to Col-0 untreated cells as determined by two-way
 753 ANOVA followed by Tukey's multiple comparisons test.



754 **Figure 3. ACC-increased ROS accumulation precedes root hair initiation.** (A) Representative images
755 of epidermal PO1 fluorescence in untreated Col-0 and Col-0 treated with ACC for 2 or 4h. Scale bar is
756 100 μm . White brackets indicate zone 2 of the root. (B) Quantification of trichoblasts that had not yet
757 formed root hair bulges of control and 2h ACC treated seedlings. (C) Quantification of number of
758 initiated root hairs in zone 2 of the root (500 μm -1000 μm from root tip) in untreated and 2 and 4h ACC-
759 treated seedlings. Data are mean \pm SEM of individual cells from 3 independent experiments (n= 12-18
760 seedlings/experiment). Columns with different letters indicate statistical significance compared to
761 untreated hair cells as determined by Student's t-test ($p < 0.0001$) in B. Columns with different letters
762 indicate statistically significant differences determined by one-way ANOVA followed by Tukey's
763 multiple comparisons test in C.



764 **Figure 4. The ETR1 receptor and EIN3/EIL1 transcription factors are required for ethylene-**
 765 **induced ROS accumulation and root hair proliferation.** (A) A schematic diagram of the ethylene
 766 signaling pathway and explanation of the character of the *etr* mutants. ETR1 (ethylene resistant 1) is the
 767 ethylene receptor controlling root hair formation, CTR1 (constitutive triple response 1 is a kinase, EIN2
 768 (ethylene insensitive 2) is a signaling protein, EIN3 and EIL1 (EIN3-like 1) are transcription factors. (B)
 769 Representative images of PO1 epidermal fluorescence in Col-0, *etr1-7*, *etr1-3*, and *ein3-leil1-1* treated
 770 with and without ACC for 4 hours. 18-20 seedlings from each genotype and treatment were imaged. Scale
 771 bar is 100 μ m. (C) Quantification of PO1 fluorescence intensity in hair cells and non-hair cells. For each
 772 root, PO1 fluorescence was quantified in two hair cells and two non hair cells and the values were pooled
 773 to obtain this average. Data are means \pm SEM of 3 experiments (n=18-20 seedlings/experiment). Columns
 774 with different letters indicate statistical significance in PO1 signal compared to other hair cells as
 775 determined by two-way ANOVA followed by Tukey's multiple comparisons test.



776 **Figure 5. ROS accumulation increases in *werewolf* and decreases in *caprice* compared to Col-0 (A)**

777 Representative images of 5-day old untreated Col-0, *cpc*, and *wer* roots stained with PO1. Scale bar is 100

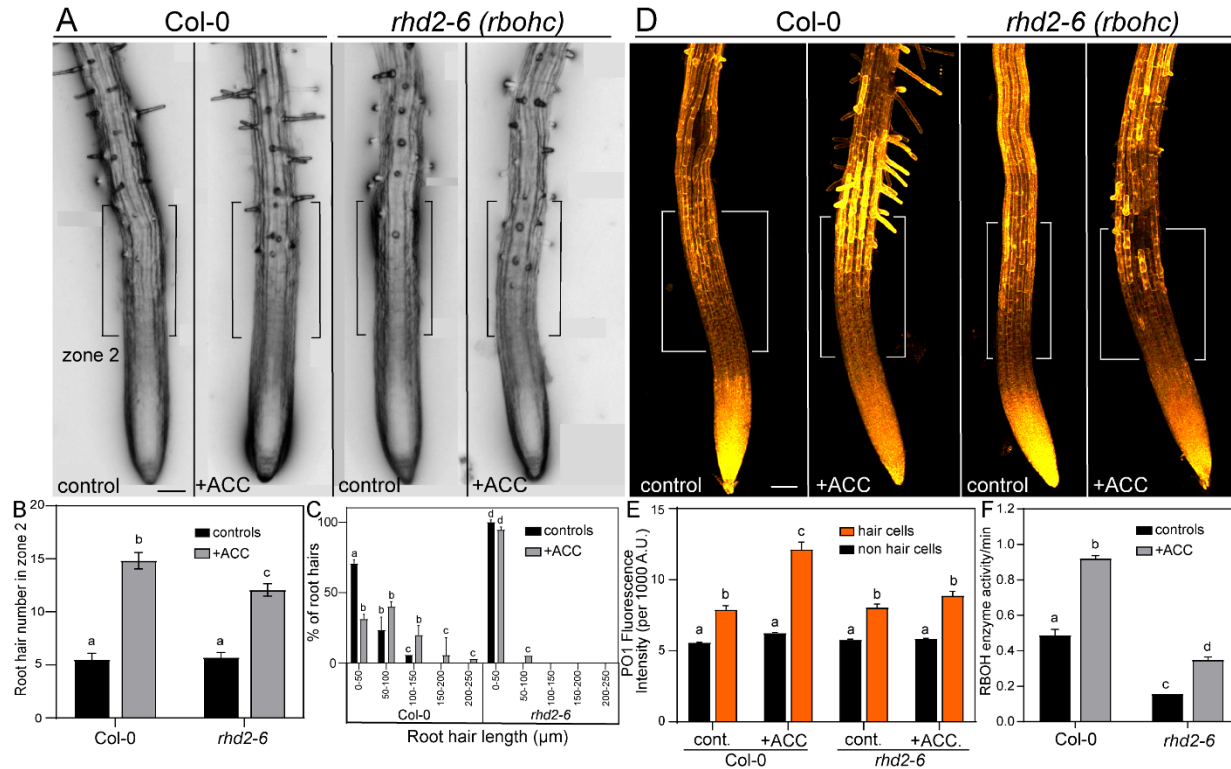
778 μm . Inset is 40x image of *wer* root to illustrate ectopic root hair formation. Scale bar = 25 μm (B)

779 Quantification of total PO1 accumulation along the root starting approximately 200 μm from the root tip

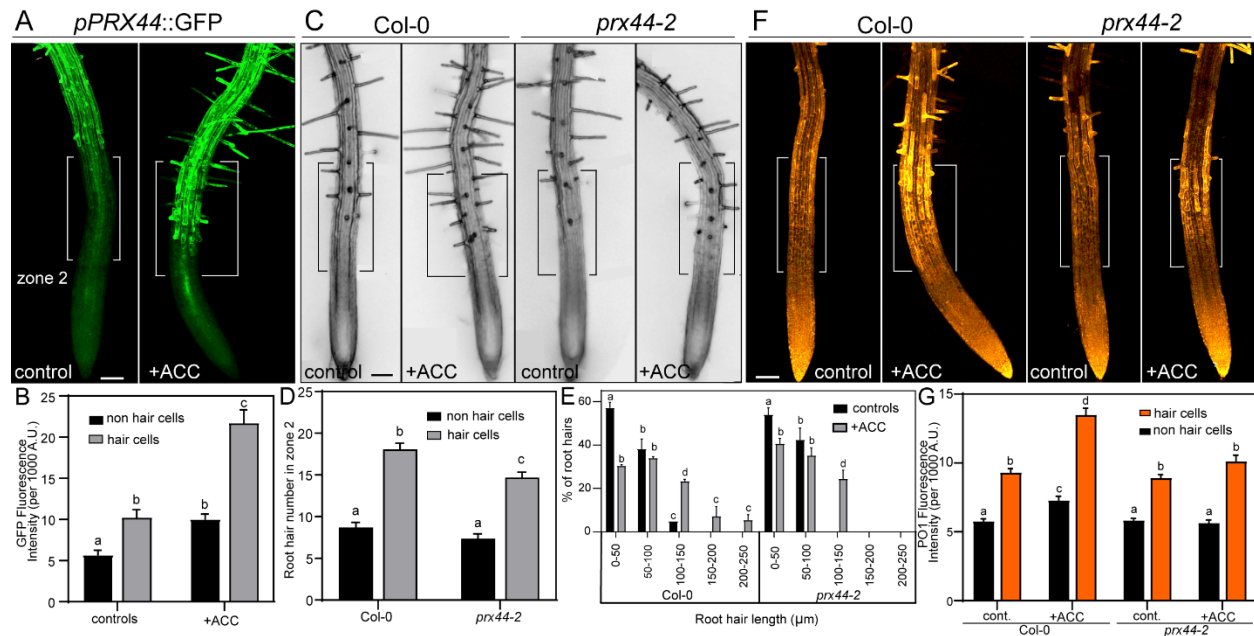
780 and ending at 1300 μm . This region encompasses both zones 2 and 3. Data are means \pm SEM and

781 representative of 2 independent experiments (9-15 seedlings per experiment). Asterisks indicate

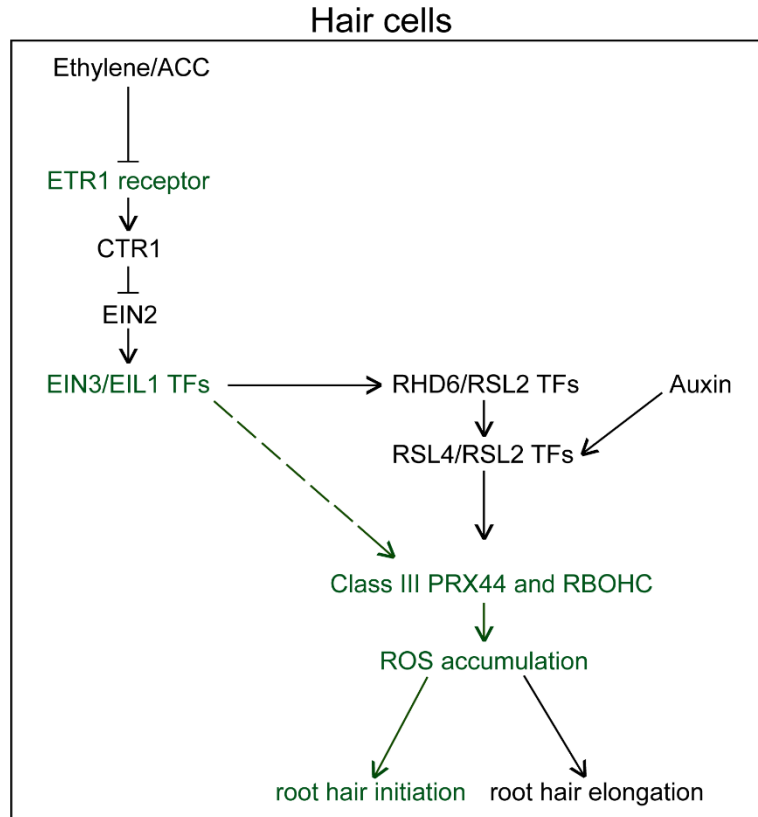
782 statistically significant differences as determined by One-way ANOVA.



783 **Figure 6. RBOHC activity contributes to ACC-induced ROS accumulation.** (A) Representative
784 images of root hairs of Col-0 and *rhd2-6* (*rbohC*) treated with and without ACC for 4 hours. Black brackets
785 indicate zone 2 of the root. (B) Root hair quantification of untreated and 4h ACC treated seedlings. Data
786 are means \pm SEM of total RH in zone 2 from 3 experiments (n=18-24 seedlings per experiment).
787 Columns with different letters indicate statistically significant differences determined by two-way
788 ANOVA followed by Tukey's multiple comparisons test. (C) Quantification of percent of root hairs
789 within a certain micron length of Col-0 and *rhd2-6* treated with and without ACC. Columns with different
790 letters indicate statistically significant differences determined by two-way ANOVA followed by Tukey's
791 multiple comparisons test. (D) Representative images of PO1 epidermal fluorescence in Col-0 and *rhd2-6*
792 treated with and without ACC for 4 hours. White brackets indicate zone 2 of the root. (E) Quantification
793 of PO1 fluorescence intensity in hair cells and non-hair cells. For each root PO1 fluorescence was
794 quantified in two hair cells (cells 1 and 5 from Figure 2) and two nonhair cells (cells 2 and 4 from Figure
795 2) and the values pooled to obtain this average. Data are the means \pm SEM of 3 experiments (n=18-24
796 seedlings/experiment). Columns with different letters indicate statistical significance in PO1 signal
797 compared to other hair cells as determined by two-way ANOVA followed by Tukey's multiple
798 comparisons test. (F) Quantification of RBOH activity as reported as changes in formazan concentration
799 per minute in roots of Col-0 and *rhd2-6* treated with and without ACC for 4 hours. Data are means \pm
800 SEM of 3 experiments. Columns with different letters indicate statistical significance as determined by
801 two-way ANOVA followed by Tukey's multiple comparisons test. Scale bars for all images are 100 μ m.



802 **Figure 7. *pPRX44::GFP* expression increases in roots treated with ACC and PRX44 contributes to**
 803 **ethylene-induced root hair formation and H₂O₂ accumulation in root hair cells (A)** Representative
 804 images of *pPRX44::GFP* treated with and without ACC for 4 hours. White brackets indicate zone 2 of the
 805 root. (B) Quantification of GFP signal in hair and non-hair cells of *pPRX44::GFP* treated with and without
 806 ACC. Data are means ± SEM (C) Representative images of RH number in Col-0 and *prx44-2* treated with
 807 and without ACC for 4 hours. Black brackets indicate zone 2 of the root. (D) Root hair quantification of
 808 untreated and 4h ACC treated seedlings. Data are means ± SEM. of 3 independent experiments (n=18-24
 809 seedlings per experiment). Columns with different letters indicated statistically significant differences
 810 determined by two-way ANOVA followed by Tukey's multiple comparison test. (E) Quantification of
 811 percent of root hairs within a certain length for Col-0 and *prx44-2* treated with and without ACC. Columns
 812 with different letters indicate statistically significant differences determined by two-way ANOVA followed
 813 by Tukey's multiple comparisons test. (F) Representative images of Col-0 and *prx44-2* treated with and
 814 without ACC for 4 hours and stained with PO1. White brackets indicate zone 2 of the root. (G)
 815 Quantification of PO1 accumulation in hair and non-hair cells of Col-0 and *prx44-2* treated with and without
 816 ACC for 4 hours (n=12-18 seedlings per experiment). For each root PO1 fluorescence was quantified in
 817 two hair cells (cells 1 and 5 from Figure 2) and two nonhair cells (cells 2 and 4 from Figure 2) and the
 818 values pooled to obtain this average. Data are means ± SEM of 3 experiments. Columns with different
 819 letters indicate statistical significance compared to all other hair cells as determined by two-way ANOVA
 820 followed by Tukey's multiple comparisons test. Scale bars for all images are 100 µm.



821 **Figure 8. Summary of mechanisms by which ethylene and auxin modulate ROS and root hair**
822 **formation.** In hair cells, ethylene, acting through the ETR1 receptor and the canonical ethylene signaling
823 pathway induces accumulation of EIN3/EIL1 TF proteins. Previous work has shown that EIN3/EIL1
824 physically interacts with RHD6/RSL2 TFs to induce expression of RSL4/RSL2 transcripts leading to root
825 hair elongation (Feng et al., 2017). It has also been shown that RSL4/RSL2 is induced by auxin signaling
826 and that RSL4/RSL2 binds to the promoters of RBOH and class III PRX genes to induce transcript
827 expression and root hair elongation (Mangano et al., 2017). Here, highlighted in green, we have shown that
828 ethylene signaling through ETR1 and EIN3/EIL1 induces ROS accumulation through RBOHC enzyme
829 activity and PRX44 transcript expression to drive root hair initiation.